Design and fabrication of two-dimensional deterministic aperiodic photonic lattices by optical induction

F. Diebel[a], M. Boguslawski[a], Nemanja M. Lučić[b], Dragana M. Jović Savić[b], and C. Denz[a]

[a]*Institut für Angewandte Physik and Center for Nonlinear Science (CeNoS), Westfälische Wilhelms-Universität Münster, 48149 Münster, Germany*

[b]*Institute of Physics, University of Belgrade, P.O. Box 68, 11001 Belgrade, Serbia*

ABSTRACT

Light propagation in structured photonic media covers many fascinating wave phenomena resulting from the band structure of the underlying lattice. Recently, the focus turned towards deterministic aperiodic structures exhibiting distinctive band gap properties. To experimentally study these effects, optical induction of photonic refractive index landscapes turned out to be the method of choice to fabricate these structures. In this contribution, we present a paradigm change of photonic lattice design by introducing a holographic optical induction method based on pixel-like spatially multiplexed single-site nondiffracting Bessel beams. This technique allows realizing a huge class of two-dimensional photonic structures, including deterministic aperiodic golden-angle Vogel spirals, as well as Fibonacci lattices.

Keywords: Photonic lattices, Aperiodic structures, Vogel spirals, Fibonacci lattices, Optical induction

1. INTRODUCTION

Designing the optical properties of materials by tailoring their band structures is an active field of research and has led to groundbreaking developments in various fields of optics [1]. These so-called photonic crystals exhibit characteristic response properties, including complete photonic band gaps, a key requirement for exciting effects and applications, e.g., band gap optical waveguides or lasing structures [2,3]. Recently, the focus of realizing spatial band gap structures turned towards deterministic aperiodic structures showing distinctive band gap properties. Due to the lack of rotational and translation symmetry, these aperiodic structures offer more isotropic band diagrams which makes complete band gaps more easy to achieve. In particular, the golden angle Vogel spiral has attracted much attention since its topology remarkably differs from many other lattices, implying effects like optical angular momentum-bearing discrete diffraction [4]. However, fabrication of these kind of structures is challenging and mostly relies on point-by-point methods which up to now excluded generation with the most prominent method: optical induction of photorefractive index landscapes. In the past, the complexity of the achievable structures has continuously increased [5,6], nevertheless these approaches rely on extended nondiffracting beams and thus are not capable to fabricate 2d deterministic aperiodic structures.

In this contribution, we present a new holographic optical induction method based on spatially multiplexed nondiffracting Bessel beams, thereby allowing for the first time longitudinal extended point-by-point techniques implemented in the optical induction of photorefractive index landscapes. This technique allows us to realize a huge class of two-dimensional photonic structures, including deterministic aperiodic golden-angle Vogel spirals as well as Fibonacci lattices.

2. DESIGN OF PHOTONIC STRUCTURES FOR OPTICAL INDUCTION

Photonic structures can be created by various methods that modulate the refractive index at small scales. The most exciting techniques are based on light itself to alter the materials properties. Besides direct femtosecond laser writing in silica glass [7,8] and two-photon-initiated polymerization [9], optically induced lattices in nonlinear refractive index materials, especially photorefractive media [10–12] are widely used. These photonic lattices represent an ultimate testbed to study fundamental linear and nonlinear physics in model experiments, confirmed by

Author to whom correspondence should be addressed. Electronic mail: falko.diebel@uni-muenster.de

Advanced Fabrication Technologies for Micro/Nano Optics and Photonics VIII, edited by Georg von Freymann, Winston V. Schoenfeld, Raymond C. Rumpf, Proc. of SPIE Vol. 9374, 93740T · © 2015 SPIE
CCC code: 0277-786X/15/$18 · doi: 10.1117/12.2080113

many convincingly demonstrated phenomena.[10,13–15]. Photorefractive structures are based on a reconfigurable light-induced refractive index modulation, which are caused by an internal electric space charge field resulting from the redistribution of the charge carriers due to illumination of the medium with the modulated light field intensity. The resulting refractive index therefore mimics the light distribution, with small deviations due to the directional mobility of the charge carriers. Because in general light is creating the refractive index lattice in which subsequently light is propagating, this concept is known as "light is guiding light".

For periodic structures this optical induction method has proven its powerful ability to create a huge variety of linear and nonlinear photonic lattices,[6,16] and over the years the structural complexity of the realized photonic lattices was developed from two-dimensional periodic[6,10] to quasi-periodic three-dimensional[17] geometries. Moreover, by transferring the concept of incoherent multiplexing known from holographic data storage to optical induction, the realization of multiperiodic superlattices[18,19], defect lattices[20], and asymmetric ratchet-like structures[21] becomes possible and further proves the flexibility of the optical induction approach in general. However, all these approaches rely on coherent or incoherent superposition of spatially extended nondiffracting beams with a high amount of regularity[6,22].

Although the diversity of these photonic lattices is impressive, a number of advanced, especially non-periodic structures cannot be fabricated with this actual tool set of optical induction. Consequently, we have further refined these methods to be capable of fabricating a wider class of two-dimensional photonic refractive index landscapes[23,24], including aperiodic structures as will be shown in the following sections.

2.1 Two-dimensional deterministic aperiodic structures

Structures at the interface between regularity and disorder are deterministic aperiodic structures[4]. These exciting intermediate states combine features of both, periodic and random structures, that are distinctive photonic band diagrams[1] on the one hand, and effects from the wide field of disordered photonics[25] on the other, together allows for molding the flow of light in completely new ways.

Regular photonic lattices show a high amount of symmetry and thus require dedicated methods to be realized with a sufficient refractive index contrast that results in a complete photonic band gap. Reducing the amount of periodicity, quasiperiodic photonic lattices with higher rotational symmetries are known to offer more isotropic band diagrams.[26] Moreover, considering deterministic aperiodic structures, which show no rotational nor translation symmetries, the realizations of complete band gap materials becomes more readily achievable.[4]

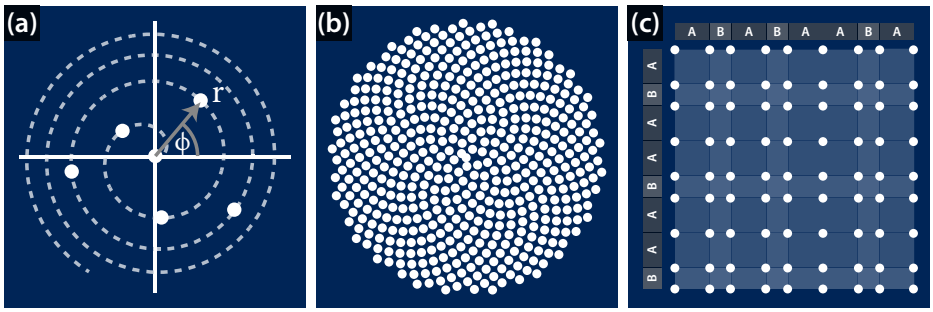

Figure 1: Two-dimensional deterministic aperiodic structures. (a) Illustration of the construction for the Vogel spiral. (b) Sketch of a typical golden-angle Vogel spiral for $N = 500$. (c) Schematic of a two-dimensional Fibonacci pattern.

Vogel spirals: Among the wide class of aperiodic structures, bio-inspired ones are most attractive because they mimic biological relevant light propagation features. One particular aperiodic pattern that shows these features is the golden angle spiral, a structure that belongs to the wider class of Vogel spirals[27] whose remarkable properties have been studied in many different fields of science. In optics, applications range from enhanced light-matter coupling designs[4] and optical angular momentum encoding schemes[28] to studies about soliton propagation in the nonlinear regime[29].

A schematic of a typical aperiodic Vogel spiral is shown in Figs. 1(a,b). The construction rule for the Vogel spiral is given by the quantization of the radial and angular variables as:

$$r = r_0\sqrt{n} \qquad \text{and} \qquad \varphi = \alpha n, \tag{1}$$

with $n = 0 \dots N$. Here, N is the number of individual sites, r_0 is a scaling factor and α is an angle which is incommensurable to π. In Fig. 1(a) the construction for the case of $N = 6$ is illustrated. For the two cases presented in this contribution, α is set to be the golden angle and its half, respectively. The golden angle is given by $\Psi = 2\pi/\Phi^2$, where $\Phi = (1 + \sqrt{5})/2$ is the golden ratio, which can also be approximated by Fibonacci numbers f_n as $\Phi = \lim_{n\to\infty} f_n/f_{n-1}$ [4].

Fibonacci lattices: Approaching from the mathematical side, the Fibonacci lattice often is referred to as the embodiment of irregularity [30,31] and numerous experiments and theoretical considerations were realized in order to discover the secrets of aperiodic media in more detail by means of Fibonacci structures [32–35]. There are different ways to construct Fibonacci lattices. Here we design it by varying the distance of adjacent waveguides in terms of sections of the Fibonacci word, different ones for the two orthogonal directions. [36]

The Fibonacci word $\mathcal{W}$ is a binary sequence where, according to the Fibonacci series, the n^{th} word is generated by putting together the two previous ones, such as

$$\mathcal{W}_n = [\mathcal{W}_{n-1}\mathcal{W}_{n-2}]. \tag{2}$$

By defining the first two words $\mathcal{W}_0 = A$ and $\mathcal{W}_1 = AB$, all following words are determined. Here, we defined two different waveguide distances A and B, with $B = A/\Phi$ where $\Phi = (1 + \sqrt{5})/2$ is the golden ratio. The first 5 Fibonacci words read as

$$\begin{aligned} \mathcal{W}_0 &= A, \\ \mathcal{W}_1 &= AB, \\ \mathcal{W}_2 &= ABA, \\ \mathcal{W}_3 &= ABAAB, \\ \mathcal{W}_4 &= ABAABABA. \end{aligned} \tag{3}$$

For the particular design of our Fibonacci lattice, we pick two subwords with a length of N from a very long Fibonacci word $\mathcal{W}_n$ with $n \gg N$, starting with a different element. Accordingly, we receive an $N \times N$ quasiperiodic, non-symmetric structure of waveguide with different distances, as depicted in Fig. 1(c). One typical characteristic of the Fibonacci word is that the probability of the two states is not equal, but the golden ratio. The distance A is more probable than B, as the probability for B is 0.62, and this bears typical structure groups: quad, double and single waveguide elements.

2.2 Principles of the pixel-wise Bessel beam induction scheme

To overcome the already mentioned restriction of optical induction to a subset of two-dimensional structures, we introduced a paradigm shift in optical lattice design: we perform the transition from parallel, spatially extended induction schemes to sequential, pixel-wise ones [23]. The main idea behind this approach is to use zero-order Bessel beams as basic entities to approximate aperiodic structures. Therefore, we place the nondiffracting Bessel beams at the transverse positions of all sites of the addressed two-dimensional structure and consider the intensity distribution resulting from incoherent superposition of all beams for the actual optical induction.

Figure 2 illustrates this basic idea exemplarily for the case of a Vogel spiral consisting of only 5 sites. If a small Gaussian beam (Fig. 2(c)) is located at each site, the ideal pattern as shown in 2(a) would result. But this light field would strongly diffract (cf. Fig. 2(f)) and thus not be suitable for the realization of two-dimensional photonic structures. Instead, locating zero-order Bessel beams of corresponding transverse size (Fig. 2(d),(e)) at each position, an intensity pattern as shown in 2(b) will result. Due to the unavoidable side lobes of the Bessel beams the resulting total intensity also shows small additional intensity modulation, but in contrast to an equally sized Gaussian beam (Fig. 2(f)), the Bessel beam (Fig. 2(g)) stays almost unchanged over the whole distance

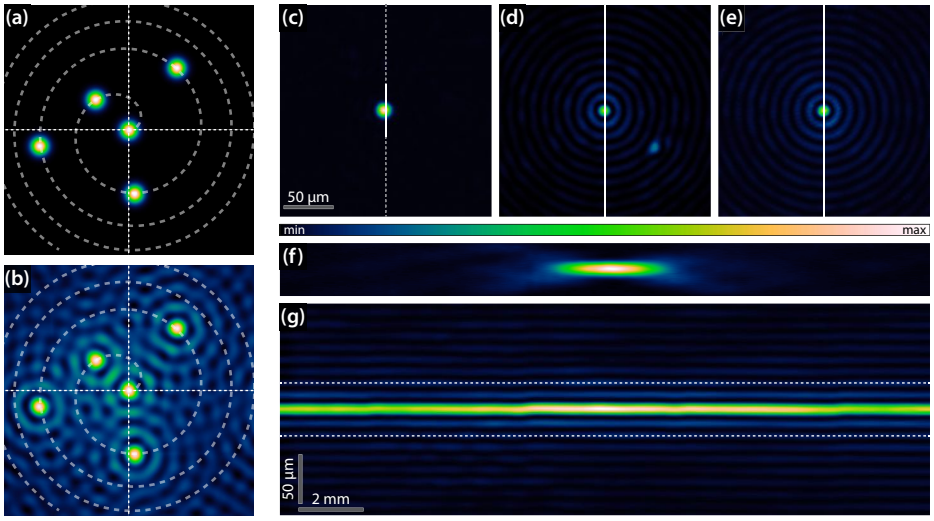

Figure 2: Principles of the pixel-wise optical induction method using multiplexed Bessel beams. (a),(b) Vogel spiral with $N = 5$ convoluted with a small Gaussian and Bessel beams, respectively. (c) Experimental intensity distribution of the corresponding Gaussian beam. (d),(e) Intensity of the Bessel beam in two transverse planes separated by $L = 20\,\mathrm{mm}$. (f) Diffraction of the Gaussian beam; cross section through the experimentally recorded three-dimensional intensity volume along the line drawn in (c). (g) Nondiffracting propagation of the experimentally realized Bessel beam.

of 20 mm and provides a nondiffracting intensity distribution to induce one single two-dimensional waveguide. The panels (a) and (b) in Fig. 2 are numerical calculations, while (c)–(g) are actual experimental results. The realized zero-order Bessel beam has a main lobe size of $w \approx 8\,\mu\mathrm{m}$ (FWHM).

Within this approach, it is crucial to superpose the individual Bessel beams incoherently and thus loosing the phase relation between them. In the opposite case, where the phase relation is preserved, interference will lead to additional undesired transverse intensity modulations. The difference between the coherent and incoherent superposition of 5 Bessel beams that resembles the inner part of Vogel spiral is shown in Fig. 3(a),(b). It is obvious that interference significantly changes and destroys the desired intensity distribution and needs to be avoided.

To bypass this interference, we illuminate the sample with the individually positioned Bessel beams one after the other in a fast sequence, which is repeated multiple times. This approach is illustrated in Fig. 3. The experimentally recorded individual Bessel beam intensities are shown in (d1)–(d5), whose incoherent superposition leads to the effective overall intensity distribution shown in Fig. 3(e). For the optical induction we utilize that the buildup of the refractive index modulation is accumulative with time, which is one of the properties of the used photorefractive material. Consequently, the multiplexing approach is expected to have the same effect on the induced refractive index modulation as a continuous illumination with an effective two-dimensional intensity pattern which would result from incoherent superposition all nondiffracting Bessel beams. For this assumption to hold, it is important to ensure an illumination time of each Bessel beam that is small compared to the typical intensity dependent dielectric relaxation time of the crystal, which is in the order of tens of seconds for the used single beam intensities of approximately 2.2 µW.[18]

Figure 3(c) shows a sketch of our setup used to perform the experiments. The beam from a frequency-doubled, continuous-wave Nd:YVO_4 laser emitting at a wavelength of $\lambda = 532\,\mathrm{nm}$ illuminates a high-resolution, programmable phase-only spatial light modulator (SLM). This modulator, in combination with two lenses and a Fourier mask, is used to set up the nondiffracting Bessel beam by addressing a pre-calculated phase pattern for each Bessel beam at its distinct position onto the SLM. This allows to computer-control every single Bessel beam's position in the transverse plane. Each beam then illuminates a 20 mm long photorefractive $Sr_{0.60}Ba_{0.40}Nb_2O_6$ (SBN:Ce) crystal which is externally biased with a dc electric field of $E_{\mathrm{ext}} \approx 2000\,\mathrm{V\,cm^{-1}}$ applied along the

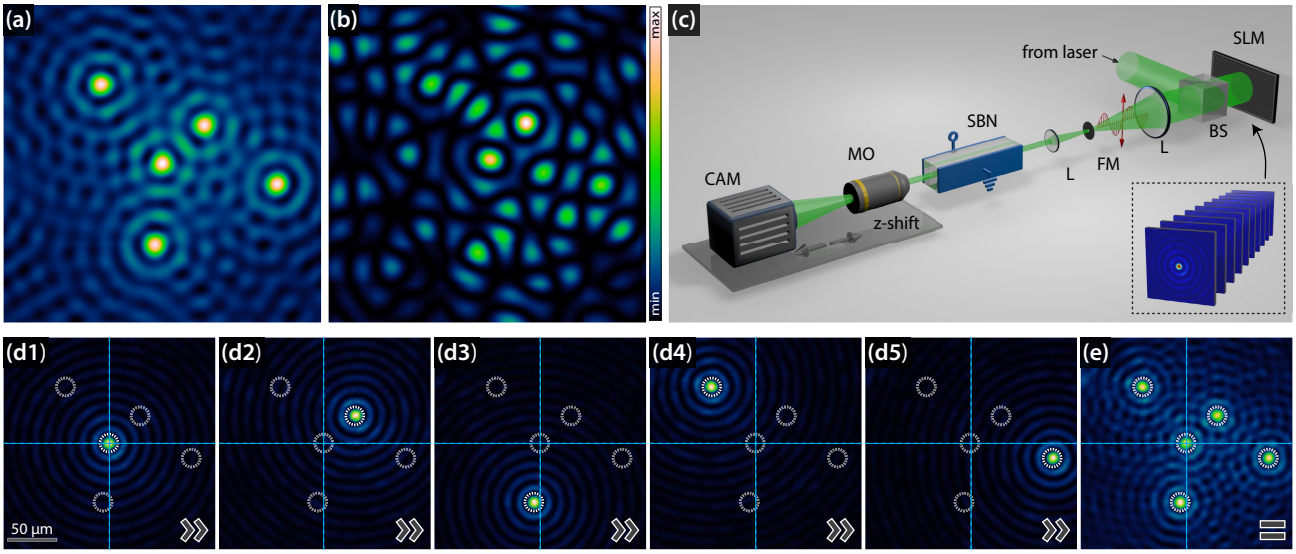

Figure 3: Details of the pixel-wise optical induction method. (a) Incoherent superposition of 5 Bessel beams, (b) coherent superposition in contrast. (c) Experimental setup. (d) Experimentally recorded intensity distribution of 5 individual Bessel beams. (e) Effective intensity by summation.

optical c-axis. With an imaging lens and a camera mounted on a translation stage the intensity distribution can be recorded in different transverse planes along the longitudinal axis.

3. EXPERIMENTAL FABRICATION OF APERIODIC PHOTONIC STRUCTURES

The introduced fabrication approach is not limited to structures consisting of only few waveguides as described above for illustration reasons. The multiplexing scheme can readily be scaled up to a considerable number of single waveguides and large, complex two-dimensional photonic structures. To demonstrate the capabilities of this pixel-wise method we demonstrate the actual optical induction of a two-dimensional golden-angle and half-golden-angle Vogel spiral with $N = 100$ single waveguides, as well as the realization of a two-dimensional Fibonacci lattice of 9×9 waveguides.

3.1 Golden-angle and half-golden-angle Vogel spiral

To realize the spatially extended two-dimensional Vogel spirals we use the corresponding number of individual zero-order Bessel beam with a main lobe size of $w \approx 8\,\mu\text{m}$ (FWHM) is shown in Fig. 2(d),(e),(g). It displays the beam intensity at the front (d) and the back face (e) of the crystal, as well as a scan along the whole crystal length of $L = 20\,\text{mm}$ (g). Following the multiplexing idea, the nonlinear photorefractive SBN crystal is now illuminated successively with all Bessel beams, each exposing the crystal for $t = 0.8\,\text{s}$. The whole sequence is repeated 30 times.

Figure 4 shows the experimentally obtained intensity profiles that will be used for the induction of the half-golden-angle spiral (Fig. 4(a)) and the golden-angle spiral (Fig. 4(b)). Figures 4(a1),(b1) and (a2),(b2) show an overlay of the experimentally realized Bessel beam intensities of the spirals at the front and the back face of the crystal, respectively. To get a better impression of the accurate spatial placement of the beams an intensity overlay $I_{\text{tot}} = (\sum_n I_n^p)^{1/p}$, with $p = 4$ of all individually recorded intensities (I_n) is shown, while the insets in Figs. 4(a2),(b2) display the resulting effective intensity as digital summation of all single intensities (with $p = 1$).

We verify the nondiffracting nature of this light field structure in longitudinal direction by plotting the intensity profile extracted from the recorded three-dimensional intensity volume along a spiral path in the transverse plane. The spiral path, shown in Fig. 4(b1), is given by the construction rule of the Vogel spiral and thus intersects all intensity peaks. For the first 10 Bessel beams along the spiral the intensity distribution is unreeled

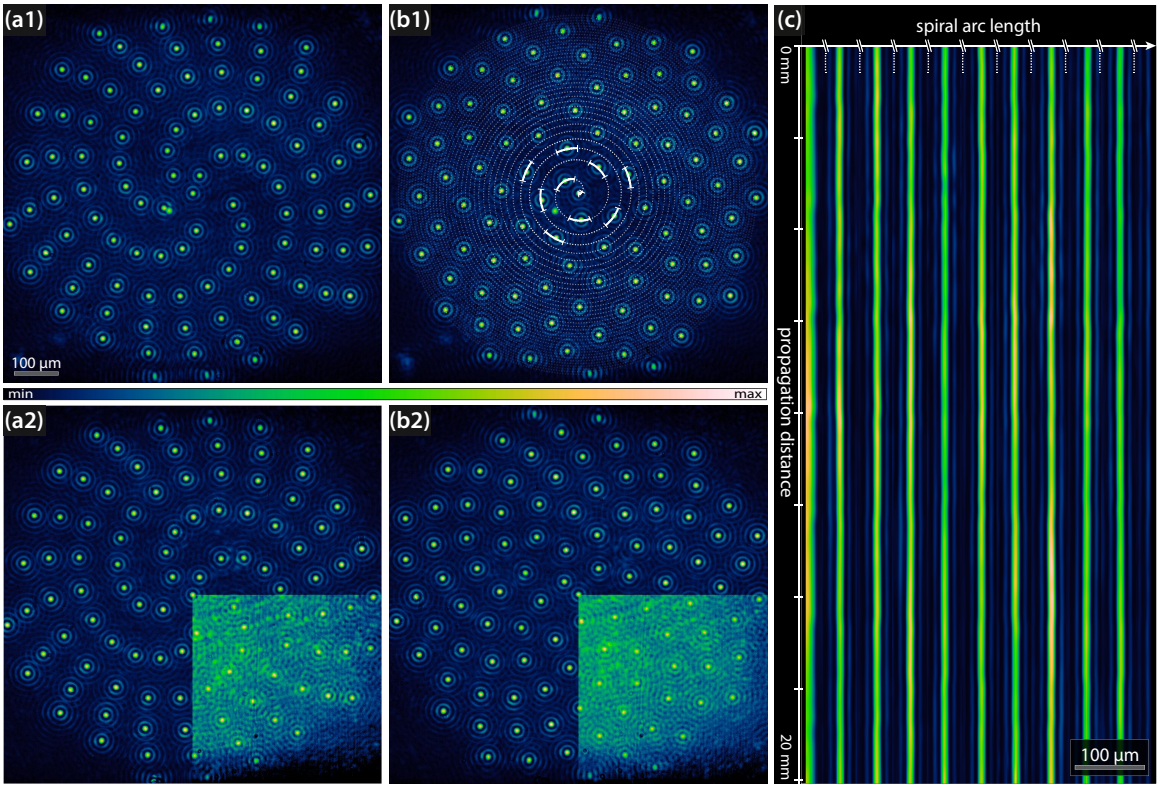

Figure 4: Two-dimensional Vogel spirals. (a1),(a2) Intensity of a half-golden-angle spiral at the front and back face of the crystal. (b1),(b2) The same for a golden-angle spiral. (c) Unreeled two-dimensional intensity cross section through the three-dimensional volume along the spiral depicted in (b1). The insets in (a2) and (b2) show the digital superposition of the intensities (with $p = 1$).

into the two-dimensional map displayed in Fig. 4(c). The straight lines clearly verify, that all beams propagate without diffracting or changing their relative distances over the whole length of the crystal.

In the final step, we transferred the resulting effective intensities via optical induction into a photonic refractive index structure. To verify that the desired structure is actually written, we illuminate the crystals front face with a plane wave after the induction is completed. The inscribed index modulation will guide and redistribute the initial homogeneous intensity to be locally increased in regions of higher refractive index. Therefore, we are able

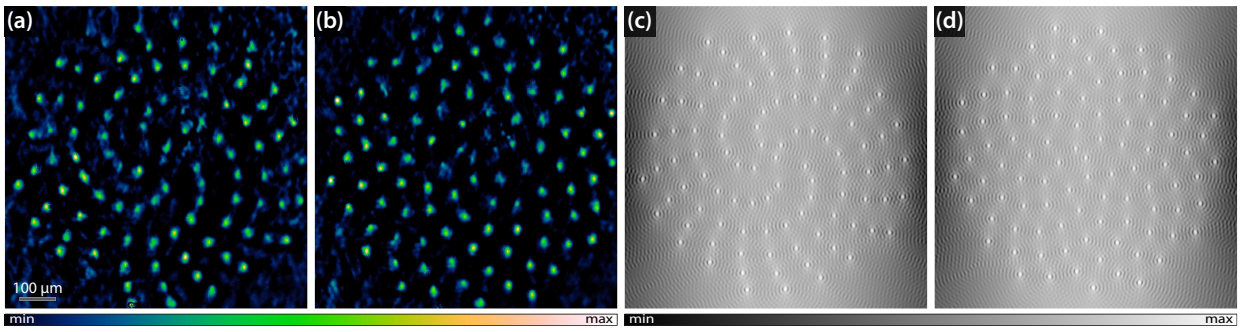

Figure 5: Optically induced refractive index modulation. (a),(b) Intensity distribution at the back face of the crystal for a plane wave propagated through the golden-angle and the half-golden-angle spiral, respectively. (c),(d) Corresponding numerically calculated refractive index modulations.

to infer the induced refractive index modulation from the intensity profile that can be recorded at the output face of the crystal. Figures 5(a) and (b) show the intensity profile of the guided waves for the half-golden-angle and the golden-angle, respectively. They clearly indicate, that the desired two-dimensional Vogel spiral structure is written with a high precision of the individual waveguide positions. For comparison, the numerically calculated refractive index modulation in the full anisotropic model[37] is shown in Figs. 5(c) and (d).

3.2 Fibonacci lattice

As a second example to demonstrate the flexibility of the proposed approach we realize a 9×9 aperiodic, two-dimensional Fibonacci structure.[36] The distances between the individual waveguides is set to be $A = 42\,\mu\text{m}$, and following $B = 26\,\mu\text{m}$. With the typical statistics for the probability of the both elements A and B of the Fibonacci word, this leads to a averaged waveguide distance and effective lattice constant of $32\,\mu\text{m}$. The size of the used Bessel beams is optimized to result in an effective intensity with as less deviation from the ideal Fibonacci lattice as possible. The main lobe size is $w \approx 10\,\mu\text{m}$ (FWHM). For the optical induction we use a similar, but shorter SBN crystal with $L = 15\,\text{mm}$, which is externally biased with the same electric dc field of $E_{\text{ext}} \approx 2000\,\text{V}\,\text{cm}^{-1}$.

The experimentally achieved effective intensity pattern I_{tot} for the optical induction of the Fibonacci lattice is shown Fig. 6(a). After induction, this structure is also probed with a plane wave to visualize the induced refractive index modulation. The guided plane wave at the output of this structure is shown in Fig. 6(b). It clearly indicates, that the corresponding Fibonacci lattice is inscribed, but does not resemble the complete resolution of the structure. The reason for this is, that due to the perpendicularly incident plane wave, the guided modes of the waveguide that are only separated by B merge and appear as only one spot. For comparison, next to these experimental results numerical calculations of the effective intensity distributions are shown. For the case, that each structure site is approximated with a zero-order Bessel beam, the numerical calculation provides the intensity shown in Fig. 6(c), which is in very good agreement to the experimentally realized counterpart (cf. (a)). Figure 6(c) illustrates the idealized case where a Gaussian beam is places at each lattice site.

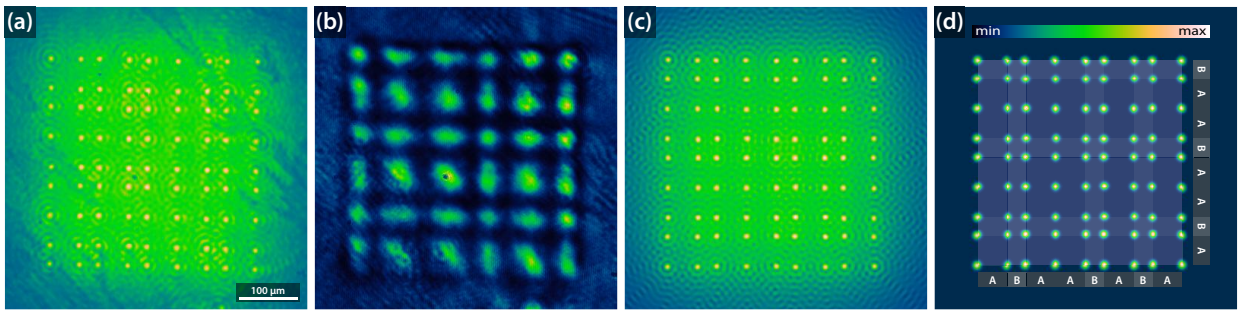

Figure 6: Optical induction of two-dimensional Fibonacci lattice. (a) Experimentally realized effective intensity for optical induction. (b) Intensity profile of the guided wave. (c) Numerically calculated intensity corresponding to (a). (d) Idealized case, where a Gaussian beam is located at each site.

4. SUMMARY

In summary, we presented a paradigm-shift in optical lattice design by introducing a holographic optical induction scheme based on pixel-wise multiplex Bessel beams. With this innovative experimental method we considerably extend the class of two-dimensional photonic lattices that now can be fabricated by optical induction, which was not possible with existing techniques. This wide class of now realizable structures contains, amongst others, deterministic aperiodic structures, structures that are of high interest for several reasons. On the one hand they exhibit new types of band diagrams useful to enhance light-matter interactions, on the other hand these aperiodic structures can be considered as an intermediate state between regular and random structures.

We have demonstrated the capabilities of this multiplexing approach by realizing both, two-dimensional golden-angle Vogel spirals, as well as Fibonacci structures. By realizing spatially extended structures which contain a considerable number of individual waveguides we further proved that this approach can easily be scaled up and is not limited to only few waveguides. Additionally, the precise adjustment of the transverse position, as well as the nondiffracting propagation of the Bessel beams and the whole structure, were proven by showing the recorded intensities in different transverse planes along the crystal.

References

[1] J. D. Joannopoulos, S. G. Johnson, J. N. Winn, and R. D. Meade, *Photonic Crystals: Molding the Flow of Light*, 2nd ed. (Princeton University Press, 2008).

[2] P. Russell, "Photonic crystal fibers." Science **299**, 358–62 (2003).

[3] H.-G. Park, S.-H. Kim, S.-H. Kwon, Y.-G. Ju, J.-K. Yang, J.-H. Baek, S.-B. Kim, and Y.-H. Lee, "Electrically driven single-cell photonic crystal laser." Science **305**, 1444–7 (2004).

[4] L. Dal Negro and S. Boriskina, "Deterministic aperiodic nanostructures for photonics and plasmonics applications," Laser Photon. Rev. **6**, 178–218 (2012).

[5] M. Boguslawski, P. Rose, and C. Denz, "Increasing the structural variety of discrete nondiffracting wave fields," Phys. Rev. A **84**, 013832 (2011).

[6] P. Rose, M. Boguslawski, and C. Denz, "Nonlinear lattice structures based on families of complex nondiffracting beams," New J. Phys. **14**, 033018 (2012).

[7] R. R. Gattass and E. Mazur, "Femtosecond laser micromachining in transparent materials," Nat. Photonics **2**, 219–225 (2008).

[8] R. Ramponi, R. Osellame, and G. Cerullo, *Springer*, Topics in Applied Physics, Vol. 123 (Springer, Berlin, 2012).

[9] H.-B. Sun, S. Matsuo, and H. Misawa, "Three-dimensional photonic crystal structures achieved with two-photon-absorption photopolymerization of resin," Appl. Phys. Lett. **74**, 786 (1999).

[10] J. W. Fleischer, M. Segev, N. K. N. Efremidis, and D. N. Christodoulides, "Observation of two-dimensional discrete solitons in optically induced nonlinear photonic lattices," Nature **422**, 147–150 (2003).

[11] D. N. Neshev, E. Ostrovskaya, Y. S. Kivshar, and W. Krolikowski, "Spatial solitons in optically induced gratings," Opt. Lett. **28**, 710 (2003).

[12] J. Petter, J. Schröder, D. Träger, and C. Denz, "Optical control of arrays of photorefractive screening solitons." Opt. Lett. **28**, 438–440 (2003).

[13] T. Schwartz, G. Bartal, S. Fishman, and M. Segev, "Transport and Anderson localization in disordered two-dimensional photonic lattices," Nature **446**, 52–55 (2007).

[14] H. Trompeter, W. Krolikowski, D. N. Neshev, A. S. Desyatnikov, A. A. Sukhorukov, Y. S. Kivshar, T. Pertsch, U. Peschel, and F. Lederer, "Bloch Oscillations and Zener Tunneling in Two-Dimensional Photonic Lattices," Phys. Rev. Lett. **96**, 053903 (2006).

[15] B. Terhalle, T. Richter, K. J. H. Law, D. Göries, P. Rose, T. J. Alexander, P. G. Kevrekidis, A. S. Desyatnikov, W. Królikowski, F. Kaiser, C. Denz, and Y. S. Kivshar, "Observation of double-charge discrete vortex solitons in hexagonal photonic lattices," Phys. Rev. A **79**, 043821 (2009).

[16] N. K. N. Efremidis, S. Sears, D. N. Christodoulides, J. W. Fleischer, and M. Segev, "Discrete solitons in photorefractive optically induced photonic lattices," Phys. Rev. E **66**, 046602 (2002).

[17] J. Xavier, M. Boguslawski, P. Rose, J. Joseph, and C. Denz, "Reconfigurable optically induced quasicrystallographic three-dimensional complex nonlinear photonic lattice structures," Adv. Mater. **22**, 356–60 (2010).

[18] P. Rose, B. Terhalle, J. Imbrock, and C. Denz, "Optically induced photonic superlattices by holographic multiplexing," J. Phys. D. Appl. Phys. **41**, 224004 (2008).

[19] M. Boguslawski, A. Kelberer, P. Rose, and C. Denz, "Multiplexing complex two-dimensional photonic superlattices." Opt. Express **20**, 27331–43 (2012).

[20] M. Boguslawski, A. Kelberer, P. Rose, and C. Denz, "Apodized structures for the integration of defect sites into photonic lattices," Appl. Phys. Lett. **105**, 111102 (2014).

[21] M. Boguslawski, A. Kelberer, P. Rose, and C. Denz, "Photonic ratchet superlattices by optical multiplexing," Opt. Lett. **37**, 797 (2012).

[22] Z. Bouchal, "Nondiffracting optical beams: physical properties, experiments, and applications," Czechoslov. J. Phys. **53**, 537–578 (2003).

[23] F. Diebel, P. Rose, M. Boguslawski, and C. Denz, "Optical induction scheme for assembling nondiffracting aperiodic Vogel spirals," Appl. Phys. Lett. **104**, 191101 (2014).

[24] F. Diebel, D. Leykam, M. Boguslawski, P. Rose, C. Denz, and A. S. Desyatnikov, "All-optical switching in optically induced nonlinear waveguide couplers," Appl. Phys. Lett. **104**, 261111 (2014).

[25] D. S. Wiersma, "Disordered photonics," Nat. Photonics **7**, 188–196 (2013).
[26] P.-T. Lee, T.-W. Lu, J.-H. Fan, and F.-M. Tsai, "High quality factor microcavity lasers realized by circular photonic crystal with isotropic photonic band gap effect," Appl. Phys. Lett. **90**, 151125 (2007).
[27] H. Vogel, "A better way to construct the sunflower head," Math. Biosci. **44**, 179–189 (1979).
[28] L. Dal Negro, N. Lawrence, and J. Trevino, "Analytical light scattering and orbital angular momentum spectra of arbitrary Vogel spirals," Opt. Express **20**, 18209 (2012).
[29] Y. V. Kartashov, V. A. Vysloukh, and L. Torner, "Solitons in spiraling Vogel lattices," Opt. Lett. **38**, 190 (2013).
[30] D. Levine and P. J. Steinhardt, "Quasicrystals: A new class of ordered structures," Phys. Rev. Lett. **53**, 2477 (1984).
[31] G. Gumbs and M. K. Ali, "Dynamical maps, Cantor spectra, and localization for Fibonacci and related quasiperiodic lattices," Phys. Rev. Lett. **60**, 1081 (1988).
[32] W. Gellermann, M. Kohmoto, B. Sutherland, and P. Taylor, "Localization of light waves in Fibonacci dielectric multilayers," Phys. Rev. Lett. **72**, 633 (1994).
[33] L. Dal Negro, C. J. Oton, Z. Gaburro, L. Pavesi, P. Johnson, A. Lagendijk, R. Righini, M. Colocci, and D. S. Wiersma, "Light transport through the band-edge states of Fibonacci quasicrystals." Phys. Rev. Lett. **90**, 055501 (2003).
[34] E. L. Albuquerque and M. G. Cottam, "Theory of elementary excitations in quasiperiodic structures," Phys. Rep. **376**, 225 (2003).
[35] Y. Lahini, R. Pugatch, F. Pozzi, M. Sorel, R. Morandotti, N. Davidson, and Y. Silberberg, "Observation of a Localization Transition in Quasiperiodic Photonic Lattices," Phys. Rev. Lett. **103**, 013901 (2009).
[36] M. Boguslawski, N. M. Lučić, D. V. Timotijević, C. Denz, and D. M. Jović Savić, "Light propagation in optically induced Fibonacci lattices," (2015), arXiv:1501.04479 .
[37] A. A. Zozulya and D. Z. Anderson, "Propagation of an optical beam in a photorefractive medium in the presence of a photogalvanic nonlinearity or an externally applied electric field," Phys. Rev. A **51**, 1520–1531 (1995).